MCSCF Study of the Cycloaddition Reaction between Ketene and Ethylene

Fernando Bernardi,[†] Andrea Bottoni,*[,†] Michael A. Robb,[‡] and Alessandro Venturini[†]

Contribution from the Dipartimento di Chimica "G. Ciamician" dell'Università di Bologna, Via Selmi 2, 40126 Bologna, Italy, and Department of Chemistry, King's College London, Strand, London WC2R 2LS, U.K. *Received September 1, 1988*

Abstract: In this paper we describe the results obtained in an MCSCF study at the STO-3G and 4-31G computational levels of the cycloaddition reaction between ketene and ethylene to form cyclobutanone. For this reaction, we have explored both the possibility of a concerted supra-antara approach between the two molecules (in agreement with the most common assumption on the mechanism of this reaction) and the possibility of nonconcerted reaction paths involving diradical species. The results obtained at the two computational levels are in good agreement and show the following: (i) One can obtain the cyclobutanone product through two possible mechanisms that have very similar energies. The energetically more favored mechanism is a highly asynchronous process (two-stage) involving the formation of a short-lived diradical intermediate. This mechanism corresponds to the attack of the ethylene molecule on the carbon atom bonded to oxygen, with the approaching direction lying in the plane of the ketene molecule (parallel approach). The other possible mechanism is a two-step process corresponding to an attack of the ethylene on the same carbon atom but with the approaching direction lying in a plane orthogonal to the plane of the ketene molecule (perpendicular approach). (ii) No reaction path exists for the supra-antara approach. The only critical point located in this case is a second-order saddle point (SOSP) that has no chemical meaning. This finding contradicts the common assumption that ketene molecules add as antarafacial partners to suprafacial olefins.

In the last few years we have begun a systematic study of the potential energy surfaces for various types of cycloaddition reactions. This study has been carried out at the ab initio MCSCF level, and the results obtained for prototype [2 + 2], [4 + 2], and 1,3 dipolar cycloadditions have recently been published.[1]

In this paper we report the results obtained in a similar study for the cycloaddition of ketene with ethylene. This reaction can be considered as a prototype example of an important class of cycloadditions, i.e., those between cumulenes and olefins. This class of reactions represents an important synthetic tool because the reactions provide a simple way to obtain cyclic compounds otherwise difficult to prepare.[2]

A large amount of experimental work has been performed on this reaction.[2-15] This work has shown the general preference of ketene to react with olefins through the C–C double bond rather than the carbonyl group. Thus, the usual products of this reaction are cyclobutanones instead of oxetanes. Only under extreme conditions, when the ketene molecule is substituted with strong withdrawing groups as in bis(trifluoromethyl)ketene, the formation of the oxetane product has been observed.[16]

This reaction is also of significant theoretical interest. According to the Woodward–Hoffmann rules this reaction can be described as a [2s + 2a] process, with the olefinic reactant participating in a suprafacial way and ketene in an antarafacial way involving the two orthogonal π-orbital systems.[17] However, even though a [2s + 2a] concerted mechanism seems to agree with the stereochemical[11,13-15] and kinetic[8] evidence, other mechanisms are possible, such as two-stage and two-step mechanisms occurring at the various centers and in the two orthogonal planes of ketene. These mechanistic possibilities have recently assumed greater interest, as a consequence of recent MCSCF results that have shown that the only critical point located for a [2s + 2a] approach of the two molecules is not a real transition state but a second-order saddle point (SOSP).[1f] A SOSP is a point on the potential energy surface that has no chemical significance, and consequently this result suggests that a supra-antara path does not exist for this type of reaction.

In contrast with the large amount of experimental work, the potential energy surface of this reaction has never been fully explored before by appropriate computational techniques, and only a few papers have been published where perturbative studies are mainly reported.[18] Only Burke, in a recent paper,[19] has partly investigated this reaction surface using a minimal STO-3G and an extended 6-31G basis set and the RHF–SCF method improved with a CI of 55 configurations. Unfortunately, the results so obtained cannot be considered really conclusive because he has not used full-optimization techniques for locating the various critical points on the surface and has not determined their nature by a computation of the corresponding Hessian matrix.

Thus, we thought it was worthwhile to examine carefully at the MCSCF level the whole potential energy surface associated

[†] Università di Bologna.
[‡] King's College London.

(1) (a) Bernardi, F.; Bottoni, A.; McDouall, J. J. W.; Robb, M. A.; Schlegel, H. B. *Faraday Symp. Chem. Soc.* **1984**, *19*, 137. (b) Bernardi, F.; Bottoni, A.; Robb, A. M.; Schlegel, H. B.; Tonachini, G. *J. Am. Chem. Soc.* **1985**, *107*, 2260. (c) Tonachini, G.; Schlegel, H. B.; Bernardi, F.; Robb, M. A. *J. Mol. Struct. THEOCHEM.* **1986**, *138*, 221. (d) McDouall, J. J. W.; Robb, M. A.; Niazi, V.; Bernardi, F.; Schlegel, H. B. *J. Am. Chem. Soc.* **1987**, *109*, 4642. (e) Bernardi, F.; Bottoni, A.; Robb, M. A.; Field, M. J.; Hillier, I. H.; Guest, M. F. *J. Chem. Soc., Chem. Commun.* **1985**, 1052. (f) Bernardi, F.; Bottoni, A.; Venturini, A.; Robb, M. A.; Field, M. J.; Hillier, I. H.; Guest, M. F. *J. Am. Chem. Soc.* **1988**, *110*, 3050. (g) Bernardi, F.; Bottoni, A.; Olivucci, M.; Robb, M. A.; Schlegel, H. B.; Tonachini, G. *J. Am. Chem. Soc.* **1988**, *110*, 5993.
(2) For reviews: Holder, R. W. *J. Chem. Educ.* **1976**, *53*, 81. Ghosez, L.; O'Donnel, M. J. *Pericyclic Reactions*; Marchand, Lehn, R. E., Eds.; Academic Press: New York, 1976; Vol. 2.
(3) Staudinger, H. *Die Ketene*; Enke: Stuttgart, 1912.
(4) (a) Martin, J. C.; Gott, P. G.; Goodlett, W.; Hasek, R. H. *J. Org. Chem.* **1965**, *30*, 4175. (b) Martin, J. C.; Goodlett, W.; Burpitt, R. D. *J. Org. Chem.* **1965**, *30*, 4309.
(5) Huisgen, R.; Feiler, L. A.; Otto, P. *Tetrahedron Lett.* **1968**, 4485.
(6) Montaigne, R.; Ghosez, L. *Angew. Chem., Int. Ed. Engl.* **1968**, *7*, 221.
(7) Katz, T. J.; Dessau, R. *J. Am. Chem. Soc.* **1963**, *85*, 2172.
(8) Huisgen, R.; Feiler, L. A.; Binsch, G. *Chem. Ber.* **1969**, *102*, 3460.
(9) Isaacs, N. S.; Stauburg, P. F. *Chem. Commun.* **1970**, 1061.
(10) (a) Brady, W. T.; Roe, R. *J. Am. Chem. Soc.* **1970**, *92*, 4618. (b) Brady, W. T.; Roe, R. *J. Am. Chem. Soc.* **1971**, *93*, 1662.
(11) Rey, M.; Roberts, S.; Dieffenbacher, A.; Dreiding, A. S. *Helv. Chim. Acta* **1970**, *53*, 417.
(12) Baldwin, J. E.; Kopecki, J. A. *J. Am. Chem. Soc.* **1970**, *92*, 4868.
(13) Brady, W. T.; Parry, F. H., III; Roe, R.; Hoff, E. F. *Tetrahedron Lett.* **1970**, 819.
(14) Brook, P. R.; Harrison, J. M.; Duke, A. J. *Chem. Commun.* **1970**, 589.
(15) Duncan, W. G.; Weyler, W., Jr.; Moore, H. W. *Tetrahedron Lett.* **1973**, 4391.
(16) England, D. C.; Krespan, C. G. *J. Org. Chem.* **1970**, *35*, 3312.
(17) Woodward, A. B.; Hoffmann, R. *The conservation of Orbital Symmetry*; Verlag-Chemie and Academic Press: Weinheim, 1970.
(18) (a) Houk, K. N.; Strozier, R. W.; Hall, J. A. *Tetrahedron Lett.* **1974**, 897. (b) Houk, K. N.; Munchausen, L. L. *J. Am. Chem. Soc.* **1976**, *98*, 937.
(19) Burke, L. A. *J. Org. Chem.* **1985**, *50*, 3149.

0002-7863/90/1512-2106$02.50/0

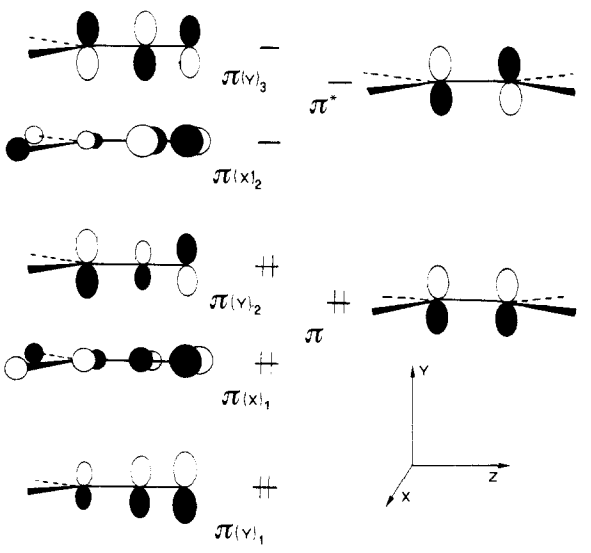

Figure 1. π orbitals of ketene and ethylene.

with this reaction in order to obtain clear information about the possible reaction mechanisms.

Computational Methods

All the computations reported in this paper have been carried out at the MCSCF level[20] with a minimal STO-3G[21] and a split-valence 4-31G[22] basis set. Integral and derivative calculations have been carried out with the GAUSSIAN 82 series of programs.[23]

At both computational levels the geometries of the various critical points of the potential surface have been optimized in the complete set of internal coordinates with an MCSCF gradient procedure.[24] Furthermore, each critical point has been characterized by diagonalization of the corresponding Hessian matrix computed at the STO-3G level with the method of finite differences. In some cases, for the structures corresponding to the most relevant critical points of the surface, the STO-3G computation of the second-derivative matrix has been carried out analytically.[25] Furthermore, we have estimated the Hessian matrices at the 4-31G level, using an updating procedure of the STO-3G Hessian matrices during the geometry optimizations.

In all cases a full-valence CI space (CASSCF) has been used for the expansion of the wave function. The initial orbitals of the valence (active) space have been obtained from the isolated fragments (i.e., ketene and ethylene at infinite separation) and are shown in Figure 1. The choice of the valence space has been dictated by the following considerations: (i) In this reaction we are describing the breaking and forming of two bonds; thus, we need four active orbitals in the plane where the reaction is taking place. (ii) Since in ketene there are two possible π planes (the yz and xz planes), we must take four orbitals from ketene and two from ethylene. (iii) Even if ketene has six π electrons and two π systems (i.e., a π_{CO} system with the $\pi(x)1$ orbital doubly occupied and the $\pi(x)2$ vacant and a π_{CCO} system with the $\pi(y)1$ and $\pi(y)2$ orbitals doubly occupied and $\pi(y)3$ vacant), we do not need to include in the valence space the first-occupied MO of the yz plane ($\pi(y)1$ orbital). This is due to the fact that since the MCSCF optimizes the orbitals, it will always find the correct subset of four orbitals of ketene. The remaining orbital will have occupancy 2.0 and will be in the core subspace. This behavior has been already verified in previous studies of other textbook cycloaddition reactions.[1e,f] For this reason the orbitals that we have included in the valence space are the $\pi(y)2$, $\pi(y)3$, $\pi(x)1$, and $\pi(x)2$ orbitals of ketene and the π and π^* orbitals of ethylene.

At the various interfragment distances of intermediates and transition state, the valence space has been obtained by orthogonalizing the active orbitals of the two isolated molecules. For each point investigated on the potential surface, the MCSCF procedure is able to keep the correct active-orbital space during the geometry optimization. The MCSCF treatment does not require any Fock matrix diagonalization with reordering of the optimized orbitals with respect to energy levels, so there is no possibility that geometry distortion can cause a swapping between a valence orbital, characterized by a variable occupancy, and a core or virtual orbital, which have occupancies 2.0 and 0.0, respectively.

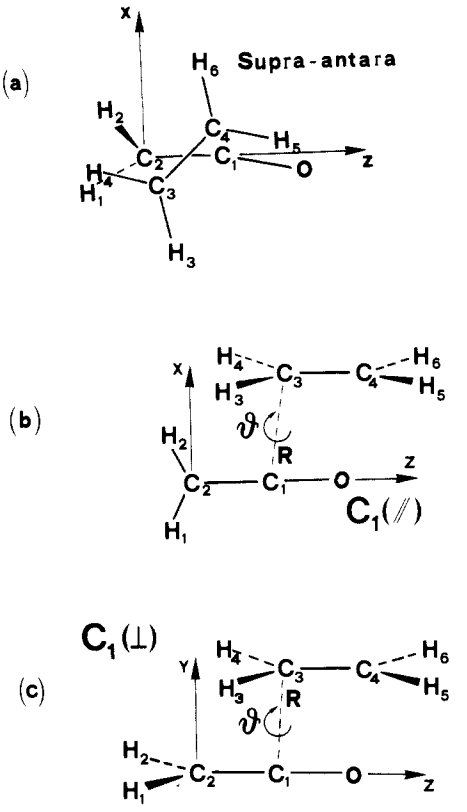

Figure 2. Schematic representation of the supra-antara approach (a), the C1($/\!/$) approach (b), and the C1($\perp$) approach (c) between ketene and ethylene.

For studying the reaction surface, we have used the following procedure that we have already described elsewhere. We have first investigated the potential surface using the minimal STO-3G basis set; then, we have used the split-valence 4-31G basis set to recompute the geometry and energy of the most important critical points located at the minimal level.

This type of computational approach can be justified on the basis of the results that we have obtained in previous work where we have studied other cycloaddition reactions.[1] In all cases we had found that the number and nature of the various critical points do not change when we explore the surface at both the minimal and split-valence basis sets. The major difference between the two computational levels is that the minimal basis set normally overestimates the stability of diradicaloid intermediates with respect to the corresponding fragmentation transition states so that the diradicaloid region becomes very flat when we use the split-valence basis. For this reason the relative energies of the various diradical species may be quite incorrect at the minimal basis set, and consequently, it becomes important to explore the most important regions of the surface also at a more accurate level.

Results and Discussion

Using the computational procedure described in the previous section, we have investigated the possibilities of both concerted approaches (in particular the supra-antara approach involving simultaneously the two orthogonal $\pi(x)$ and $\pi(y)$ orbital systems) and various nonconcerted approaches (which entail the formation of diradicaloid species). These approaches are schematically represented in Figures 2 and 3 where the notation used to define the internal coordinates is also given.

To denote the various attacks and the corresponding reaction paths (with the exception of the supra-antara one), we have distinguished between "parallel" approaches ($/\!/$ symbol), which occur in the plane of the ketene molecule (xz plane), and "perpendicular" approaches ($\perp$ symbol), which occur in the yz plane, which is orthogonal to the ketene molecule. Thus, the

(20) (a) Hegarty, D.; Robb, M. A. *Mol. Phys.* **1979**, *38*, 1795. (b) Robb, M. A.; Eade, R. H. A. *NATO Adv. Study Inst. Ser., Ser. C* **1981**, *67*, 21.
(21) Hehre, W. J.; Stewart, R. F.; Pople, J. A. *J. Chem. Phys.* **1969**, *51*, 2657.
(22) Ditchfield, R.; Hehre, W. J.; Pople, J. A. *J. Chem. Phys.* **1971**, *54*, 724.
(23) GAUSSIAN 82: Carnegie Mellon University, Binkley, J. S.; Whiteside, R. A.; Krshnan, R.; Seeger, R.; De Frees, D. J.; Schlegel, H. B.; Topiol, S.; Kahn, L. R.; Pople, J. A.
(24) Schlegel, H. B.; Robb, M. A. *Chem. Phys. Lett.* **1982**, *93*, 43.
(25) Robb, M. A.; Schlegel, M. A., to be published.

Table I. Total Energy Values (E_t) and Energy Differences (ΔE_t and $\Delta E_t'$) of the Various Critical Points Obtained for the Cycloaddition Reaction between Ketene and Ethylene at the STO-3G and 4-31G Computational Levels

	STO-3G			4-31G		
critical points[a]	E_t[b]	ΔE_t[c]	$\Delta E_t'$[c]	E_t[b]	ΔE_t[c]	$\Delta E_t'$[c]
			C1(∥) Approach			
C1(∥)g TS	−226.872 91	18.72	25.35	−229.430 68	0.45	53.33
C1(∥)g M	−226.902 75	0.00	6.65	−229.431 39	0.00	52.89
C1(∥)g′ TS	−226.898 56	2.63	9.25	−229.428 54	1.78	54.67
C1(∥)t SOSP	−226.867 69	22.00	28.63			
			C1(⊥) Approach			
C1(⊥)t TS	−226.868 06	21.77	28.45	−229.429 90	0.93	53.82
C1(⊥)t M	−226.893 67	5.70	12.35	−229.437 15	−3.61	49.27
C1(⊥)c TS	−226.889 02	8.62	15.27			
C1(⊥)c SOSP	−226.861 58	25.84	32.48			
			C2(⊥) Approach			
C2(⊥)g TS	−226.849 44	33.45	40.08			
C2(⊥)g M	−226.897 81	3.10	9.75			
C2(⊥)t TS	−226.849 29	33.55	40.20			
C2(⊥)t M	−226.897 92	3.03	9.68			
C2(⊥)g′ TS	−226.893 33	5.91	12.56			
C2(⊥)g″ TS	−226.897 42	3.34	9.97			
C2(⊥)c SOSP	−226.843 39	37.25	43.90			
			O(∥) Approach			
O(∥)g TS	−226.833 33	43.56	50.19			
O(∥)g M	−226.848 98	33.74	40.37			
O(∥)t TS	−226.832 34	44.18	50.81			
O(∥)t M	−226.848 97	33.75	40.37			
O(∥)g′ TS	−226.846 98	35.00	41.62			
O(∥)g″ TS	−226.848 25	34.20	40.82			
			Supra–Antara Approach			
supra–antara SOSP	−226.832 03	44.38	51.00	−229.408 87	14.13	67.02
reactants	−226.913 31	−6.65	0.00	−229.515 67	−52.89	0.00
products						
cyclobutanone	−227.012 59	−68.92	−62.27	−229.523 78	−57.97	−5.08
2-methyleneoxetane	−226.983 18	−50.46	−43.82	−229.490 84	−37.30	15.59

[a] M denotes a minimum, TS a transition state, and SOSP a second-order saddle point. [b] Values in atomic units. [c] Values in kilocalories per mole.

different modes of attack can be classified as follows.

(i) C1(∥) Approach. The formation of the first carbon–carbon bond involves one ethylene carbon atom (C3) and atom C1 of ketene, with the attack occurring in the *xz* plane that corresponds to the ketene molecular plane (see Figure 2b). This reaction path leads either to the formation of cyclobutanone or to the formation of 2-methyleneoxetane.

(ii) C1(⊥) Approach. The atoms involved in the formtion of the first C–C bond are still the two atoms C1 and C3, but the attack occurs in the *yz* plane, orthogonal to the ketene plane (see Figure 2c). Also in this case we can obtain both cyclobutanone and oxetane products.

(iii) C2(⊥) Approach. The approaching direction still lies in the *yz* plane, but the two atoms involved in the formation of the first bond are C2 and C3 (see part a of Figure 3). Only the cyclobutanone product can be obtained in this way.

(iv) O(∥) Approach. This attack occurs in the ketene molecular plane; the oxygen and the carbon C3 are the two atoms involved in the formation of the first bond (see Figure 3b).

(v) O(⊥) Approach. The formation of the first bond still involves the O and C3 atomic centers, but the attack occurs now in the *yz* plane (see Figure 3c). For both the O(∥) and O(⊥) approaches, the ring closure can only lead to the formation of the oxetane molecule.

All the relevant critical points located on the reaction surface are listed in Table I together with the corresponding total energy values (E_t) obtained at both the STO-3G and 4-31G levels. In the same table we have also reported the energy differences (ΔE_t) computed with respect to the lowest energy structure corresponding to the gauche-type minimum found for the C1(∥) approach and the energy differences ($\Delta E_t'$) computed with respect to reactants.

Furthermore, an energy profile for the two most important reaction paths C1(∥) and C1(⊥) is given in Figure 4, while schematic representations of the relevant structures together with

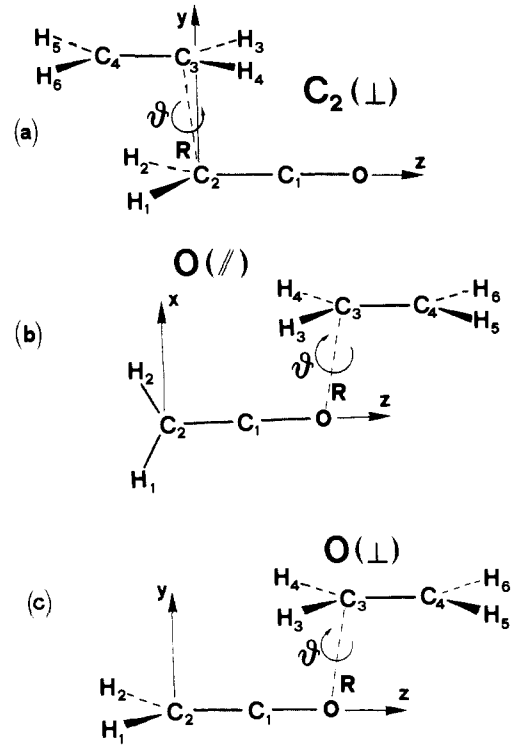

Figure 3. Schematic representation of the C2(⊥) approach (a), the O(∥) approach (b), and the O(⊥) approach (c) between ketene and ethylene.

the values of the most significant geometrical parameters are given in Figures 5–13. A complete tabulation of the optimized geo-

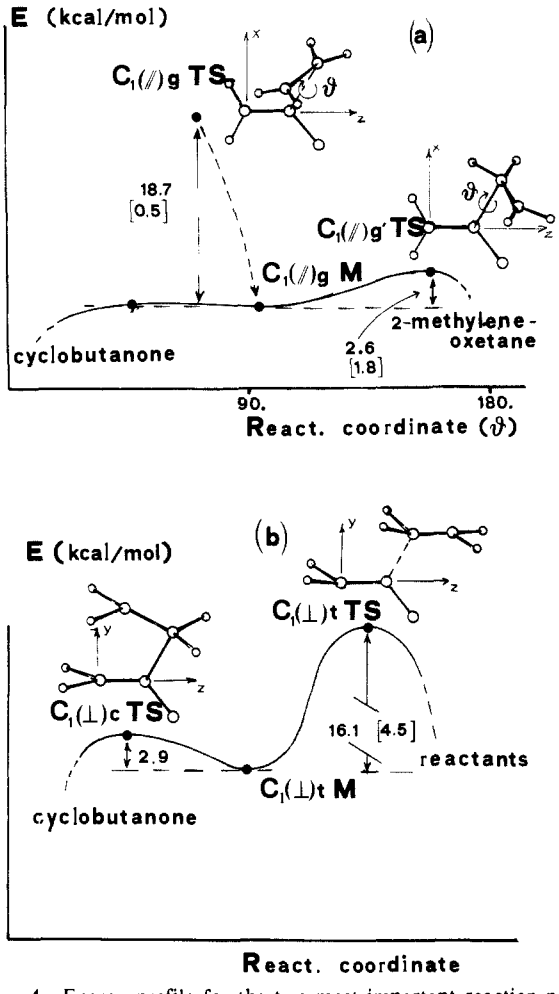

Figure 4. Energy profile for the two most important reaction paths, C1(||) and C1(⊥), computed for the ketene–ethylene cycloaddition reaction.

metrical parameters for the various structures obtained at the STO-3G and 4-31G computational levels is collected in Tables II–VII in the supplementary material. The geometries reported for the reactant and product molecules (Table VII) have been obtained at the RHF level. The notation used to define the internal coordinates is the same as that used in Figures 2 and 3.

Finally, to perform the numerical computation of the Hessian matrix at the STO-3G level for the various critical points, we have used a subspace defined by the internal coordinates that we have considered to be the most important ones for describing the reaction. These coordinates are as follows. For the C1(||) and C1(⊥) approaches: bond lengths C1–C3, C2–C1, C3–C4, and C1–O; angles O–C1–C2, C3–C1–C2, and C4–C3–C1; and dihedral angles O–C1–C2–C3, C4–C3–C1–C2, H1–C2–C1–C3, H2–C2–C1–C3, H3–C3–C4–C1, H4–C3–C4–C1, H5–C4–C3–C1, and H6–C4–C3–C1. For the C2(⊥) approach: bond lengths C2–C3, C2–C1, C3–C4, and C1–O; angles O–C1–C2, C3–C2–C1, and C4–C3–C2; and dihedral angles O–C1–C2–C3, C4–C3–C2–C1, H1–C2–C1–C3, H2–C2–C1–C3, H3–C3–C4–C2, H4–C3–C4–C2, H5–C4–C3–C2, and H6–C4–C3–C2. For the O(||) approach: bond lengths C3–O, C2–C1, C3–C4, and C1–O; angles O–C1–C2, C3–O–C1, and C4–C3–O; and dihedral angles. C2–C1–O–C3, C4–C3–O–C1, H1–C2–C1–O, H2–C2–C1–O, H3–C3–C4–O, H4–C3–C4–O, H5–C4–C3–O, and H6–C4–C3–O.

C1(||) Approach. The region of the surface corresponding to this reaction path is represented in part a of Figure 4. This region is characterized by the presence of a gauche transition state (C1(||)g TS) and a gauche minimum (C1(||)g M), schematically represented in parts a and b of Figure 5, respectively. Both structures are true diradicals, with the two unpaired electrons mainly localized on the C4 carbon atom and on the oxygen atom.

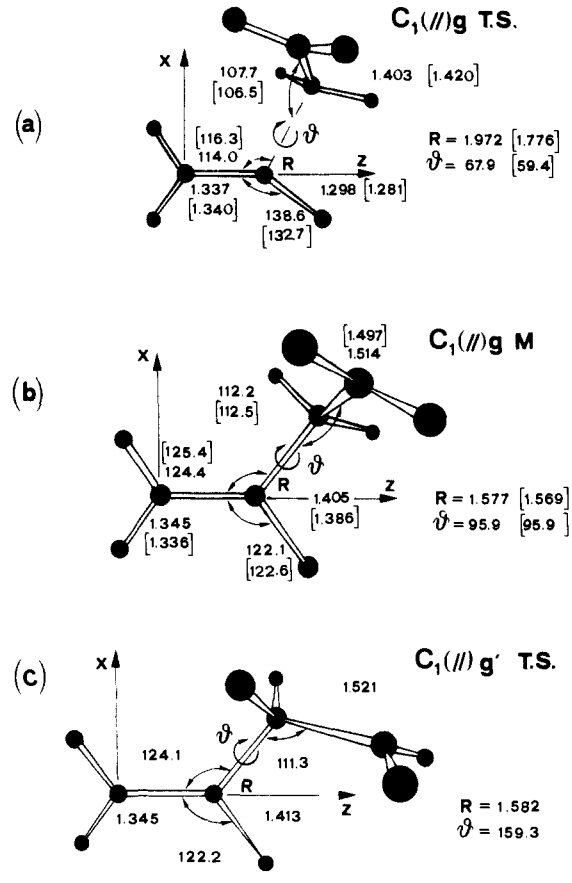

Figure 5. STO-3G and 4-31G optimized geometries for C1(||)g TS (a), C1(||)g M (b), and C1(||)g' TS (c). The 4-31G values are in brackets, lengths are in angstroms, and angles in degrees.

The Hessian matrix corresponding to the C1(||) TS (computed analytically) is characterized by only one negative eigenvalue, which proves that this critical point is a real transition state (first-order saddle point). The dominating component of the Hessian eigenvector associated with the negative eigenvalue is given by R, the approaching distance between the two molecules, showing that the C1(||) TS corresponds to the formation of the first carbon–carbon bond (the C1–C3 bond).

Inspection of Figure 5 shows that, for these two structures, the values of the geometrical parameters do not change very much in passing from the STO-3G to the 4-31G computational level. Relevant changes can be observed only for the angle θ and the approaching distance R in the case of the transition state. θ is a dihedral angle characterizing the various structures and describing the relative position of the ethylene and ketene fragments with respect to the rotation around the C1–C3 direction. The value $\theta = 0$ is taken to correspond to the situation where the C3–C4 bond eclipses the C1–C2 bond. In the present case, at the STO-3G level, we have found that the value of θ is 67.9° in C1(||)g TS and 95.9° in C1(||)g M, showing that the formation of the first bond C1–C3 is associated with a significant rotation around the direction of this bond. At the 4-31G level the value of θ does not change in the C1(||)g minimum, but becomes much smaller in the C1(||)g TS (59.4°).

Furthermore, the length of the new forming C1–C3 bond, at the STO-3G level, is 1.972 Å in the C1(||)g TS and becomes 1.577 Å in the C1(||)g M where this C–C bond is almost completed. This value remains almost unchanged at the 4-31G level in the minimum (1.569 Å) but becomes much shorter in the transition state (1.776 Å).

As a consequence of the fairly good agreement between the STO-3G and the 4-31G optimized geometries, the change in passing from the 4-31G energy values computed at the STO-3G geometry to the 4-31G energy values computed at the 4-31G geometry is quite small. It is in fact 1.34 kcal/mol for the

minimum and 1.99 kcal/mol for the transition state. Nevertheless, while at the STO-3G level the barrier between the C1(‖)g TS and the C1(‖)g M is 18.72 kcal/mol, at the 4-31G geometry this barrier becomes almost negligible (only 0.45 kcal/mol), showing that at the 4-31G level the region that corresponds to the formation of the first new bond is extremely flat. The increasing flatness of the surface and the trend observed in the geometry changes on going from the minimal to the extended basis set are both in agreement with the results already found for other reactions such as the thermal cycloaddition of two ethylenes[1b] or the Diels–Alder reaction between ethylene and butadiene.[1e,f]

We have also investigated the ring closure from the C1(‖)g minimum to oxetane and cyclobutanone. For the process that leads to oxetane, we have located a critical point (C1(‖)g′ TS, see Figure 5c) characterized by approximately the same value of the C1–C3 bond found for the minimum (1.582 Å at the STO-3G level), but by a much larger value of the rotation angle θ (159.3°). The corresponding Hessian matrix has only one negative eigenvalue with the corresponding eigenvector dominated by θ, showing that this structure is a conformational transition state that connects the gauche minimum to the 2-methyleneoxetane molecule through the rotation around the C1–C3 bond. We have found, at the STO-3G level, that the barrier for this conformational process is 2.63 kcal/mol. To evaluate the same barrier at the 4-31G level, we have performed various computations with this basis set at different values of the rotation angle θ and using the 4-31G geometry of the C1(‖)g minimum. We have found that, at this computational level, this barrier remains at the same order of magnitude, about 1.80 kcal/mol (corresponding to a value of θ of 150.0°).

On the other hand, an accurate investigation of the process leading to cyclobutanone has shown that, at both computational levels, this region of the potential surface is extremely flat, which makes impossible location of any transition state. Consequently, this process seems to occur without any significant barrier.

All the present results seem to suggest that while the less favored process leading to the oxetane product corresponds to a nonconcerted reaction path with two kinetically distinct steps (the first corresponding to the formation of the C–C bond, the second to the formation of the C–O bond), the situation is more complicated in the case of the more favored process leading to cyclobutanone. The results obtained in the latter case do not allow one to assess whether the corresponding mechanism is a two-step or a completely asynchronous (two-stage) concerted mechanism. This problem arises from the fact that the diradical intermediate C1(‖)g M, if it exists, is very short-lived, since the barrier to its conversion to cyclobutanone is negligible as we have found at both computational levels.

In addition to the approaches previously described, we have also studied the possibility of a trans approach (θ = 180°). Also in this case we have located a critical point corresponding to a structure that is characterized by a value of the C1–C3 distance equal to 1.973 Å at the STO-3G level. The corresponding Hessian matrix has two negative eigenvalues, which show that this point is a second-order saddle point (SOSP), i.e., a point on the potential surface characterized by two directions of negative curvature. Even though such a point, denoted here as C1(‖)t SOSP, has no chemical significance, it is of interest to analyze the shape of the two negative transition vectors. While the lower eigenvector is dominated by the approaching distance R, the most important component of the higher eigenvector corresponds to the rotation angle θ. These results suggest that this SOSP connects on the potential surface the two possible C1(‖)g transition states.

C1(⊥) Approach. The results obtained from the investigation of the region corresponding to this type of approach are summarized in part b of Figure 4. In this case we have located a trans transition structure C1(⊥)t TS (θ = 180°) and a corresponding trans minimum C1(⊥)t M, both diradical in nature with two unpaired electrons mainly localized on the carbon atoms C2 and C4. We have also found that the energy barrier of the transition state with respect to the minimum is about 16.07 kal/mol at the STO-3G level and 4.54 kcal/mol at the 4-31G level. The geometries of these two species are represented in parts a and b of Figure 6. Inspection of this figure shows that, also in this case, the values of the geometrical parameters computed at the two computational levels are in good agreement. The most relevant change is found again in the length of the forming bond (C1–C3) in C1(⊥)t TS, which is 1.989 Å at the STO-3G level and becomes 1.795 Å at the 4-31G level. While in the case of the minimum we have found that the corresponding Hessian matrix has all positive eigenvalues, in the case of C1(⊥)t TS only one negative eigenvalue has been obtained. The largest component in the corresponding eigenvector is given by the approaching distance R, which means that this structure is a real transition state corresponding to the formation of the first bond (the C1–C3 bond). Inspection of the total energy values obtained at the two computational levels has shown that the C1(⊥)t transition state is higher in energy than the C1(‖)g transition state. This energy difference is about 3.05 kcal/mol at the STO-3G level but becomes much smaller, only 0.48 kcal/mol, at the 4-31G level. These results suggest a possible competition between the C1(‖) and the C1(⊥) reaction paths for the formation of cyclobutanone.

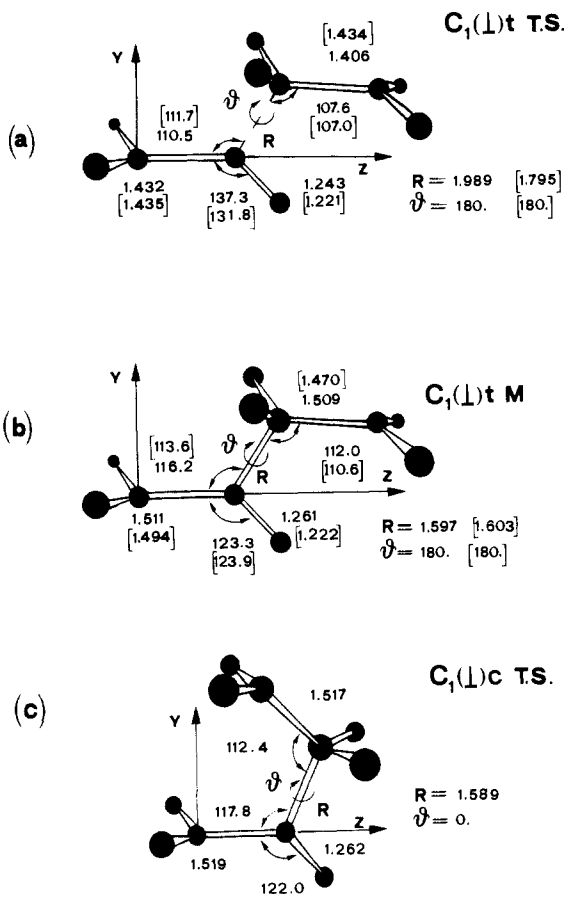

Figure 6. STO-3G and 4-31G optimized geometries for C1(⊥)t TS (a), C1(⊥)t M (b), and C1(⊥)c TS (c). The 4-31G values are in brackets, lengths are in angstroms, and angles in degrees.

In addition to the trans approach, the possibilities of both a gauche and a cis approach (the latter corresponding to a supra–supra approach of the two molecules, characterized by θ = 0.0°) have been investigated. While no structures with a value of θ intermediate between 180.0° and 0.0° (gauche-type structures) have been found, two additional structures, both characterized by the same value of θ = 0.0° (cis-type structures) but by different values of R, have been determined. The distance R, obtained at the STO-3G level, is in one case 1.589 Å and in the other case 1.974 Å. The computation of the corresponding Hessian matrices has shown that none of these two critical points are a transition state corresponding to the formation of the first C–C bond. In one case (R = 1.974 Å) the Hessian is characterized by two negative eigenvalues showing that this point is a second-order saddle point (C1(⊥)c SOSP). Inspection of the two corresponding

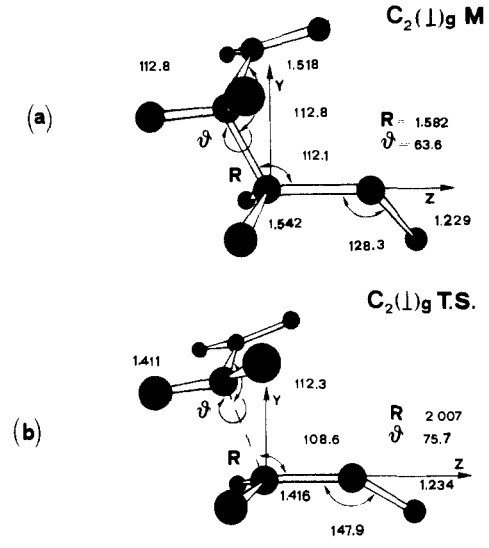

Figure 7. STO-3G optimized geometries for C2(⊥)g M (a) and C2(⊥)g TS (b). Lengths are in angstroms and angles in degrees.

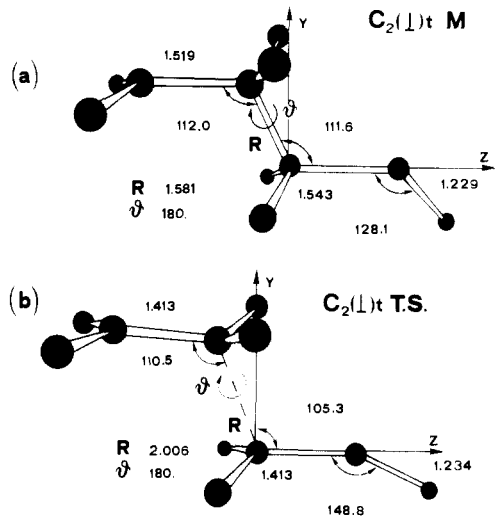

Figure 8. STO-3G optimized geometries for C2(⊥)t M (a) and C2(⊥)t TS (b). Lengths are in angstroms and angles in degrees.

eigenvectors has shown that while the first eigenvector (the lower one) is dominated by the approaching distance R, the most important component of the second eigenvector (the higher one) corresponds to the rotation angle θ. In the other case (R = 1.589 Å) the Hessian matrix has only one negative eigenvalue: The largest components of the corresponding eigenvector are in this case the rotation angle θ and the dihedral angles that define the relative orientation of the two terminal methylene groups, suggesting that this point corresponds to the transition state for the ring closure to cyclobutanone (C1(⊥)c TS) from the C1(⊥)t M. A schematic representation of C1(⊥)c TS is given in part c of Figure 6.

Finally, the possibility of ring closure to oxetane from the C1(⊥) M has been investigated, but in spite of extensive search, no transition state corresponding to this process has been found.

C2(⊥) Approach. A coplanar approach, where the ethylene C3–C4 bond eclipses the chetene C1–C2 bond (θ = 0°), and a gauche and a trans approach have been investigated.

The results show that this region of the potential energy surface is very similar to the surface of the ethylene–ethylene thermal cycloaddition reaction.[1b] In agreement with those results, for the coplanar approach we have located, at the STO-3G level, a diradical structure characterized by a value R of 2.020 Å. However, the corresponding Hessian matrix has two negative eigenvalues, indicating that this point is a second-order saddle point denoted here as C2(⊥)c SOSP. The direction of negative curvature, corresponding to the lower negative eigenvalue, is dominated by R while the other direction is dominated by the rotation angle θ and corresponds to a motion that breaks the molecular plane of symmetry.

We now discuss the results obtained for the gauche and trans approaches. Similar to the ethylene–ethylene case, using the STO-3G basis set, we have found that this region is characterized by a gauche and a trans minimum (C2(⊥)g M and C2(⊥)t M) and by a gauche and a trans transition state (C2(⊥)g TS and C2(⊥)t TS). The geometries of the two gauche structures are represented in Figure 7, and those corresponding to the two trans structures are reported in Figure 8. The computed Hessian matrix has only positive eigenvalues in the case of the two structures, which were supposed to be a minimum, and only one negative eigenvalue in the case of the two transition states. In the latter case the direction of negative curvature is dominated by the approaching distance R, showing that the two transition states correspond to the formation of the first bond C2–C3. We have also found that the values of the forming bond are 2.006 and 2.007 Å in the trans and gauche transition states, respectively, and become 1.581 and 1.582 Å in the two corresponding minima. The dihedral angle θ is 180° in the trans approach and becomes 75.7° and 63.6° in C2(⊥)g TS and C2(⊥)g M, respectively.

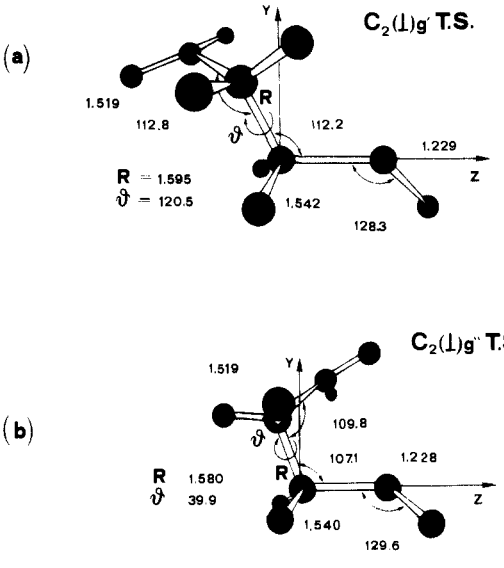

Figure 9. STO-3G optimized geometries for C2(⊥)g′ TS (a) and C2(⊥)g″ TS (b). Lengths are in angstroms and angles in degrees.

Furthermore, from the STO-3G total energy values reported in Table I, it can be seen that the two minima are almost at the same energy, with the trans slightly more stable than the gauche, the energy difference being only 0.07 kcal/mol. Similar considerations apply in the comparison between the gauche and trans transition states. The energy difference is again very small (only 0.10 kcal/mol), with the gauche slightly more stable than the trans.

It is also interesting to note that the two transition states located for the C2(⊥) approach lie much higher in energy than does C1(∥)g TS, the difference, at the STO-3G level, between the C2(⊥)t TS and the C1(∥)g TS being 14.83 kcal/mol. In order to obtain a better estimate of the relative importance of the two reaction mechanisms, on the basis of the fairly good agreement between the STO-3G and 4-31G geometries previously pointed out, we have carried out a 4-31G computation on the STO-3G optimized geometry of C2(⊥)t TS. Also at this computational level this transition structure is much higher in energy than the C1(∥)g TS (16.82 kcal/mol), suggesting that this mechanism is energetically much more disfavored than that associated with the C1(∥) and C1(⊥) approaches.

In addition to the structures previously described, two more critical points corresponding to two diradical species, denoted here as C2(⊥)g′ TS and C2(⊥)g″ TS (see Figure 9), have been found

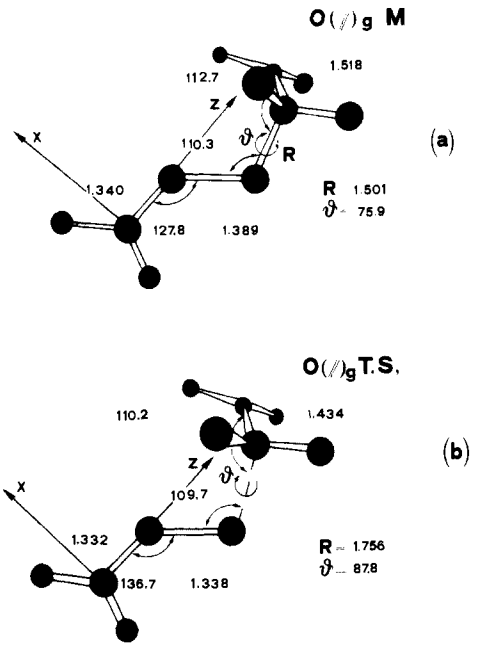

Figure 10. STO-3G optimized geometries for O(||)g M (a) and O(||)g TS (b). Lengths are in angstroms and angles in degrees.

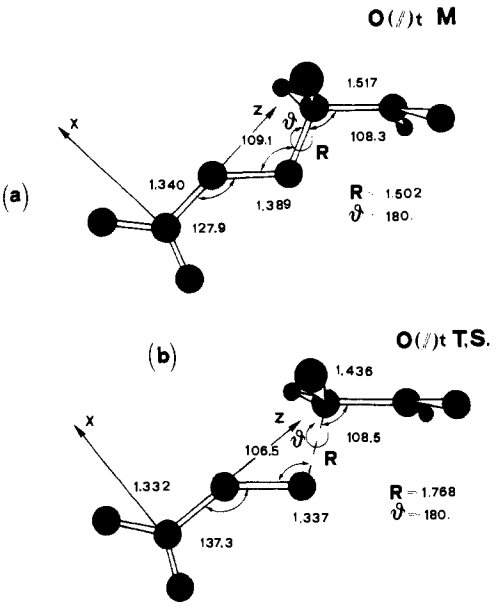

Figure 11. STO-3G optimized geometries for O(||)t M (a) and O(||)t TS (b). Lengths are in angstroms and angles in degrees.

at the STO-3G level. The values of the rotation angle θ that characterize these two structures are 120.5° in the former case (this value is intermediate between the typical values for the trans and gauche minima) and 39.9° in the latter case (intermediate between the gauche minimum and the coplanar situation). The corresponding Hessian matrices have in both cases only one negative eigenvalue, with the corresponding eigenvector dominated by the angle θ, showing that these structures are conformational transition states. In particular, the C2(⊥)g′ TS connects the trans and gauche minima, while the C2(⊥)g″ TS corresponds to the ring closure from the gauche minimum with the formation of cyclobutanone.

Inspection of the total energy values shows that, at the STO-3G level, the barrier associated with the rotation leading from C2(⊥)t M to C2(⊥)g M is about 2.9 kcal/mol, while the process leading from the gauche minimum to the cyclobutanone product occurs without almost any barrier (0.24 kcal/mol).

O(||) Approach. The region of the surface corresponding to this reaction path, which can only lead to the formation of oxetane, is very similar to that we have just discussed for the C2(⊥) approach.

Using the minimal STO-3G basis set, we have located gauche and trans minima, denoted here as O(||)g M (Figure 10a) and O(||)t M (Figure 11a), and gauche and a trans transition states, denoted as O(||)g TS (Figure 10b) and O(||)t TS (Figure 11b). The typical values of θ for these four diradicaloid structures are 180.0° and 75.9° for O(||)t M and O(||)g M and 180.0° and 87.9° for O(||)t TS and O(||)g TS, respectively.

The corresponding Hessian matrices are characterized by all positive eigenvalues in the case of the two supposed minima and by only one negative eigenvalue in the case of the two supposed transition structures. The corresponding eigenvectors, in the latter case, are dominated by the approaching distance R, which indicates that these two species represent the transition states for the formation of the C3–O bond. This bond was found to be 1.768 and 1.756 Å in the trans and gauche cases, respectively.

The total energy values collected in Table I show that both the two transition states and the two minima are approximately at the same energy, with the gauche structures slightly more stable than the trans ones. These values show also that the two fragmentation transition states are much higher in energy than the corresponding transition states located for the other approaches. At the STO-3G level, the O(||)t TS is 25.46 kcal/mol higher in energy than the C1(||)g TS. At the 4-31G level, with the STO-3G

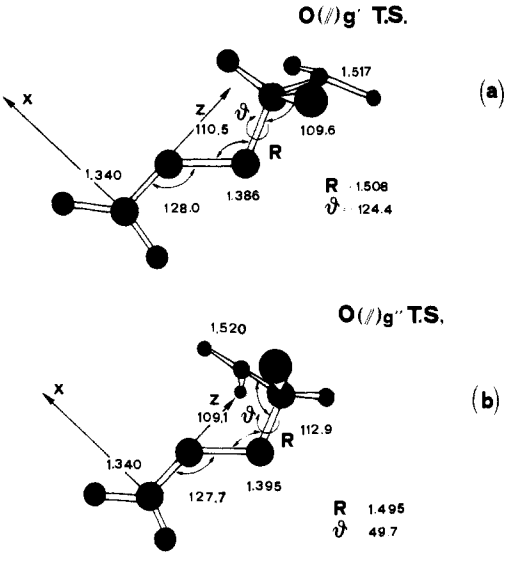

Figure 12. STO-3G optimized geometries for O(||)g′ TS (a) and O(||)g″ TS (b). Lengths are in angstroms and angles in degrees.

optimized geometry for O(||)t TS, this energy difference becomes 34.24 kcal/mol, which makes the O(||) reaction path highly disfavored with respect to the other reaction paths.

In addition to the previous structures we have also located a critical point corresponding to the conformational transition state connecting the trans minimum to the gauche minimum. This transition structure is denoted as O(||)g′ TS and is characterized by a θ of 124.4° (see Figure 12a) and by a barrier of 1.25 kcal/mol. We have also investigated the ring closure from the O(||)g M to the oxetane. We have found that this process involves an additional conformational transition state (O(||)g″ TS; see Figure 13b) corresponding to θ = 49.1° and occurring without almost any barrier (0.46 kcal/mol).

O(⊥) Approach. This region has been accurately investigated, but in spite of extensive search, no critical point has been located.

Supra–Antara Approach. A critical point has been located for the concerted "supra–antara" approach, which involves simultaneously the two orthogonal x and y π-orbital systems of the ketene molecule. The corresponding structure, together with the optimum values of the most relevant geometrical parameters, is shown in Figure 13.

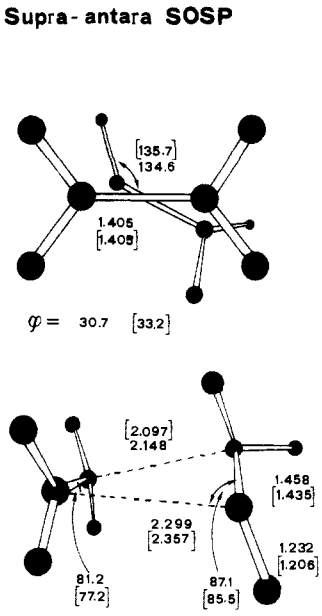

Figure 13. STO-3G and 4-31G optimized geometries for the structure located for the supra-antara approach. The 4-31G values are in brackets, ϕ denotes the dihedral angle C3-C4-C1-C2, lengths are in angstroms and angles are in degrees.

This critical point has been characterized, at the STO-3G level, by the analytical computation of the corresponding Hessian matrix. This computation has shown that this point is a second-order saddle point. It is quite interesting to analyze the shape of the two eigenvectors corresponding to the two directions of negative curvature. This analysis shows that the motion along one of the two directions leads to the cyclobutanone product, while the motion along the other direction connects the two adjacent gauche transition states C1(∥)g TS and C2(⊥)g TS. These results indicate that, for the ketene-ethylene reaction, the supra-antara path does not exist. The critical point corresponding to this approach is not a real transition structure, but a local maximum with two directions of negative curvature.

Because of the theoretical importance associated with the supra-antara approach, this point has been carefully reinvestigated at the 4-31G level. Also at this computational level we have located a critical point that, on the basis of the diagonalization of the corresponding updated Hessian matrix, is characterized again by two directions of neative curvature. The geometry of this SOSP, which lies 14.31 kcal/mol above the C1(∥)g M, is quite close to that we have computed at the STO-3G level as can be seen from the values reported in Figure 13.

Conclusions

In this paper we have described an MCSCF study of the cycloaddition reaction between ketene and ethylene performed with a minimal STO-3G and a split-valence 4-31G basis set. The results obtained at the two computational levels are in good agreement and show that for this reaction various paths exist leading to two possible products: cyclobutanone and 2-methyleneoxetane.

In particular we have found that the formation of cyclobutanone can occur through two possible mechanisms that have very similar energies. These two mechanisms are associated with a C1(∥) approach and a C1(⊥) approach: in both approaches the rate-determining step is associated with the formation of the first C–C bond, and the related transition states (C1(∥)g TS and C1(⊥)t TS) have been found to have approximately the same energy. These two transition states lead to the formation of two intermediates (C1(∥)g M and C1(⊥)t M) from which we can have the ring closure to cyclobutanone.

The structure corresponding to the C1(∥)g M seems to be a very short-lived intermediate since its conversion to cyclobutanone occurs without any barrier; this suggests that the mechanism associated with the C1(∥) approach is not a two-step mechanism but rather a concerted highly asynchronous two-stage mechanism (with the first stage corresponding to the formation of the first C–C bond and the second stage corresponding to the ring closure). This result is in accord with the concerted nature of this reaction that was proven for several cases and considered as an attribute of a [2s + 2a] process.[2-15]

Furthermore, at both computational levels, we have found that from C1(∥)g M we can also have the ring closure to oxetane through a conformational transition state (C1(∥)g′ TS). Since this process involves a barrier of about 1.8 kcal/mol at the 4-31G level (2.63 kcal/mol at the STO-3G), it is energetically less favored than the conversion to cyclobutanone, in good agreement with the experimental results, showing that the cyclobutanone rings are the main products of this type of reaction.

Investigation of the other possible reaction paths (i.e., the C2(⊥) approach, which can lead only to cyclobutanone, and the O(∥) approach, which can lead to either cyclobutanone or oxetane) has shown that they involve high-energy transition states for the formation of the first bond, which makes the corresponding mechanisms energetically more disfavored than those previously discussed.

An extensive examination of the region corresponding to a supra-antara approach has shown, at both computational levels, that this type of reaction path does not exist, the critical point that we have located being a SOSP. This result contradicts the common assumption that this reaction proceeds through a concerted reaction path of supra-antara type.

All these results do not contradict the conclusions reached by Burke,[19] who in his paper suggested that the reaction can proceed through a nonsynchronous concerted path. In addition to this nonsynchronous path we have also found that the two-step reaction path C1(⊥) can be important. This mechanism, which leads to a loss of stereospecifity, can explain the experimental data obtained in some cases (in the presence of substituents with large steric effects) that are in excellent agreement with the hypothesis of a two-step nonconcerted pathway.[15] Furthermore, we have demonstrated the importance of computing the Hessian matrix to determine the real nature of the various critical points, showing that no transition states but only SOSPs exist for a [2s + 2a] or a [2s + 2s] approach.

Finally, some comment on the accuracy of these computations is necessary. Even if these computations have been carried out with quite modest basis sets, we have some numerical evidence that the qualitative nature of the critical points will not be critically basis set dependent. For another textbook cycloaddition reaction, i.e., the ethylene–ethylene reaction, the barrier to fragmentation from the trans and gauche diradical minimum of tetramethylene has been computed at the MCSCF level with various basis sets of different accuracy.[1b] These results show that the barrier is about 10 kcal/mol at the STO-3G level and becomes less than 1 kcal/mol at the 4-31G level. The same barrier increases by ca. 1 kcal/mol with the 6-31G* basis set (Doubleday et al.[26]) and decreases again (about 1 kcal/mol)[27] with an extended Dunning basis set.[28] All these results suggest that even if these barriers are very sensitive to the basis set quality, the qualitative nature of the critical points is not affected by the changing of the basis set.

Furthermore, regarding the nature of the supra-antara SOSP, an observation can be made. As we have pointed out, the second direction of negative curvature for this critical point connects two gauche fragmentation transition states. If the supra-antara critical point was a real transition state, one should find a maximum along this coordinate (between the supra-antara point and the gauche transition state), which seems, a posteriori, quite unlikely.

Also another computational aspect, which concerns the amount of correlation energy correction included in our calculations, must be pointed out. Usually we distinguish between two different types

(26) Doubleday, C.; Page, M.; McIver, J. W. *J. Mol. Struct. THEOCHEM.* **1988**, *163*, 331.
(27) Bernardi, F.; Bottoni, A.; Olivucci, M.; Robb, M. A.; Venturini, A., to be published.
(28) Dunning, T. H., Jr. *J. Chem. Phys.* **1970**, *53*, 2823.

of correlation energy effects. The first type, the so-called nondynamic correlation, is associated with the breaking down of the Hartree–Fock model in the regions of the potential surface where we have degeneracy or near-degeneracy of several configurations. This frequently occurs in reactivity problems when we describe the rupture and formation of bonds. This problem can be solved with the MCSCF method with a limited CI expansion that includes the near-degenerate configurations. Unfortunately this approach is not capable of describing satisfactorily the second type of correlation effect, i.e., the dynamic correlation associated with the motion of electrons. To take this contribution into account, a large CI expansion is required. Nevertheless, for similar structures, like those we have found in the transition-state region, it is quite conceivable to assume that this contribution does not change very much. Thus, reliable information can be obtained by comparing these various structures (intermediates and transition states) and evaluating the relative energy barriers. These considerations also suggest that improvement in the correlation treatment should not change the qualitative nature of the potential surface. The situation is quite different when we consider the product molecules or the reactant molecules, and we try to compare them with the transition-state region. The contribution of the dynamic correlation in these three different situations will be in general quite different. Because of this, care must be taken in evaluating at this computational level the exothermicities of the reaction or in comparing the activation energies computed at the MCSCF level (see the data reported in Table I) with the experimental results. The theoretical energy of activation is about 25 kcal/mol at the STO-3G level but becomes about 53 kcal/mol at the 4-31G level. This value is too high when compared with the value of the activation energy of 32 kcal/mol[19] that can be estimated on the basis of the experimentally known gas-phase standard heats of formation of ketene, ethylene, and cyclobutanone.

Registry No. Ketene, 463-51-4; ethylene, 74-85-1.

Supplementary Material Available: Tables of optimized STO-3G and 4-31G geometrical parameters for various structures from the C1(∥) and C1(⊥) reaction paths (Tables II and III), STO-3G parameters for C2(⊥) and O(∥) reaction paths (Tables IV and V), STO-3G and 4-31G parameters for the supra–antara SOSP (Table VI), and STO-3G and 4-31G parameters for ethylene, ketene, cyclobutanone, and 2-methyleneoxatane (Table VII) (6 pages). Ordering information is given on any current masthead page.

Theoretical Interpretation of the Absorption and Ionization Spectra of the Paracyclophanes

Sylvio Canuto[†] and Michael C. Zerner*

Contribution from the Quantum Theory Project, University of Florida, Gainesville, Florida 32611. *Received December 27, 1988*

Abstract: The ultraviolet absorption spectra of the [*m*·*m*]paracyclophanes are studied by utilizing an INDO/S-CI method. The [4.4] and higher paracyclophanes can be considered as two parallel *p*-xylenes and the spectrum is interpreted as a simple doubling of the xylene bands. For the [3.3]paracyclophane the first band observed in absorption is assigned to the second excited state, $^1B_{3u}$, but with the first calculated state, $^1B_{2g}$, borrowing intensity from higher states. This lowest $^1B_{2g}$ state may be responsible for an inflection on the first observed band and it is held responsible for the emission observed in concentrated benzene solution. By utilizing di-*p*-xylene as a model system for the [*m*·*m*]paracyclophanes, the dependence of the ultraviolet absorption spectra with the interring separation is systematically analyzed. [2.2]Paracyclophane, known to have a short interring separation (3.1 Å) and a boat-like distortion of each ring, presents a spectrum that is considerably more complex. All seven bands observed experimentally are considered in our theoretical assignment (i.e. <60 000 cm^{-1}). Our calculations utilize the crystallographic structure and the results indicate that the lowest band consists of two transitions, one allowed ($^1B_{3u}$) and one forbidden ($^1B_{2g}$), borrowing intensity from a higher $^1B_{2u}$ state via the a_u vibrational mode (twisting of the rings in opposite directions around the major axis). This lowest state $^1B_{2g}$ is interpreted as responsible for the weak fluorescence and for the long axis polarized absorption. The observed phosphorescence of [2.2]paracyclophane is assigned to the emission $^3B_{3g}$–^1A_g. For the calculation of this emission energy the geometry of the excited $^3B_{3g}$ state is optimized by using the ab initio SCF gradient technique with the STO-3G basis set. The ionization spectrum of the [2.2]paracyclophane is calculated by using both the INDO/S-CI method and the ab initio SCF procedure with a split-valence basis set. The interpretation of the spectrum of the paracyclophanes presented in this paper is perhaps the most consistent so far available and conforms very well with all known experimental characteristics.

1. Introduction

The interpretation of the electronic absorption and emission spectra of systems of cofacially arrayed molecular hydrocarbons is of great importance in understanding steric and transannular resonance effects, charge transfer, and the nature of the intermolecular interaction. Among these systems cyclophanes have been of particular interest.[1] In [*m*·*n*]cyclophanes two benzene rings are held together by bridges of $(CH_2)_m$ and $(CH_2)_n$. Different inter-ring distances are associated with different values of *m* and *n*. The [*m*·*n*]cyclophanes thus provide a regular series of molecules in which the interaction of aromatic rings at varying separations can be systematically examined. In the smaller cyclophanes the two benzene rings are so close as to give rise to abnormal absorption bands that cannot be traced back to the usual

* Permanent address: Departamento de Fisica, Universidade Federal de Pernambuco, 50000 Recife PE, Brazil.

(1) (a) Cram, D. J.; Steinberg, H. J. *J. Am. Chem. Soc.* **1951**, *73*, 5691. (b) Brown, C. J. *J. Chem. Soc.* **1953**, 3265. (c) Koutecki, J.; Paldus, J. *Collect. Czech. Chem. Commun.* **1962**, *27*, 599. (d) Gleiter, R. *Tetrahedron Lett.* **1969**, *51*, 4453. (e) Boyd, R. H. *J. Chem. Phys.* **1968**, *49*, 2574. (f) Schweitzer, D.; Colpa, J. P.; Behnke, J.; Hansser, K. H.; Haenel, M.; Staab, H. A. *Chem. Phys.* **1975**, *11*, 373. (g) Schweitzer, D.; Colpa, J. P.; Hansser, K. H.; Staab, H. A. *J. Luminesc.* **1976**, *12/13*, 363. (h) Hoffman, R. *Acc. Chem. Res.* **1971**, *4*, 1. (i) Vogler, H. *Theor. Chim. Acta. (Berlin)* **1981**, *60*, 65. (j) Paddow-Row, M. N. *Acc. Chem. Res.* **1982**, *15*, 245. (k) Boekelheide, V. *Acc. Chem. Res.* **1980**, *13*, 65. (l) Voegtle, E.; Hohner, G. *Top. Curr. Chem.* **1978**, *74*, 1. (m) Hoffman, R.; Imamura, A.; Hehre, W. J. *J. Am. Chem. Soc.* **1968**, *90*, 1499.

0002-7863/90/1512-2114$02.50/0